DOI https: //doi. org/10.1007/s11595-019-2068-0

Influence of Annealing Treatment on Microstructure Evolution and Mechanical Property of Friction Stir Weld AZ31 Mg Alloys

LI Yajie[1], QIN Fengming[1], LIU Cuirong[1], LI Leijun[2], ZHAO Xiaodong[1], WU Zhisheng[1*]

(1. School of Materials Science and Engineering, Taiyuan University of Science and Technology, Taiyuan 030024, China; 2. Department of Chemical and Materials Engineering, University of Alberta, Edmonton 999040, Canada)

Abstract: In order to improve microstructure distribution and mechanical properties of Mg alloy joint by annealing treatment, die-casting AZ31 Mg alloy was successfully welded at rotation speed of 1 400 rpm and travel speed of 200 mm/min. The welded joints were annealed at 150-300 ℃ for 15-120 min and then were subjected to transverse tensile. The microstructure of annealed joints was analyzed by optical microscopy and electron backscatter diffraction. The experimental results indicate that (0001) texture intensity in stir zone significantly reduces and sharp transition of grain size is relieved in the interface between stir zone and thermo-mechanically affected zone after annealed at 200 ℃ for 30 min. Meanwhile, the elongation is increased from 7.5% to 13.0% and strength is increased slightly. It is because that annealing treatment can inhibit twin transformation and retain its ability to coordinate deformation during tensile deformation, which contributes to the improvement of plasticity. In addition, annealing treatment can increase the width of interfacial transition zone and lead to gradual transition of grain size between the SZ and TMAZ, which balances dislocation diffusion rate in different zone.

Key words: magnesium alloys; friction stir welding; annealing treatment; texture distribution; plasticity

1 Introduction

The remarkable characteristics of magnesium alloys are low density and high strength, which makes them suitable for application in transportation, aerospace and 3C industries (computer, communication and consumer electronics)[1,2]. One of the major drawbacks is low ductility for Mg alloys compared to face- or body-centered cubic Fe and Al alloys. The five independent slip systems are required for sufficient ductility by the von Mises criterion[3]. For Mg alloys, only three independent slip systems belonging to the basal plane can be activated at room temperature. However, critical stress for activating prismatic plane slip is two orders higher than basal plane slip, which results in poor ductility and limited formability of anisotropic hexagonal metals[4]. For manufacturing of some specific or complex Mg alloy structural parts, researchers gradually focus attention to new joining technologies to replace die forging and rolling technologies.

Joining magnesium alloys by conventional fusion welding techniques may result in porosity, hot cracking and grain coarsening, which can deteriorate mechanical properties and corrosion resistance of welded joints[5]. Friction stir welding (FSW) as a solid state joining process can avoid a series of defects caused by fusion welding, which is suitable for Mg alloys joining[6-8]. After FSW, the microstructure in the stir zone (SZ) is significantly changed. For example, it is found that the SZ microstructure is usually characterized by refined equiaxed grains, which has been demonstrated that this is associated with continuous recrystallization or discontinuous recrystallization and preferred orientation of (0001) basal planes during FSW[8-12]. Hence, stir zone has better strength and plasticity, which is attributed to significant grain refinement[13]. Nevertheless, FSW also can leads to formation of inhomogeneous microstructure and deformation texture in interface between stir zone and thermo-mechanically affected zone (TMAZ).

(Received: Apr. 18, 2018; Accepted: July 9, 2018)

LI Yajie(李亚杰): Ph D Candidate; E-mail: liyajie1207@ 126.com

*Corresponding author: WU Zhisheng(吴志生): Prof.; E-mail: wuzstyust@163.com

Funded by the Fund for Shanxi Key Subjects Construction, the National Natural Science Foundation of China (No. 51275332), and the Natural Science Foundation of Shanxi Province (No. 201601D011036)

The strong transition of grain size or crystal orientation from SZ to TMAZ generally causes strain localization and significantly deteriorates welding strength and ductility[9,11,14-16]. Therefore, the fracture frequently occurs in the interface between TMAZ and SZ during deformation[13]. To our knowledge, numerous studies focus on improvement of microstructure and mechanical property of FSW Mg alloys by optimizing weld parameters. In addition, some investigations reported that post-deformation can improve FSW joint strength by introducing multiple twins[17,18]. However, this method led to the reduction of the ductility of FSW joints. It is well know that post-annealing treatment for deformed materials can improve microstructure distribution depending on static recovery and recrystallization[19]. However, less systematic researches about to effect of heat treatment on microstructure evolution and tensile properties of FSW Mg alloy joints have been done.

Thus, the effect of annealing temperature and holding time on microstructure evolution and mechanical property of friction stir weld AZ31 alloys was investigated. We focus on variation of grain size, texture intensity and distribution in different zone of FSW AZ31 Mg alloys during annealing treatment. The obtained results could optimize annealing parameters and provide a valid method to improve plasticity of FSW joints.

2 Experimental

The materials are die-casting AZ31 magnesium alloy with a nominal chemical composition of Mg-3.0Al-1.0Zn (wt%). To illustrate the microstructure of base material (BM), optical micrograph of cross-section (along transverse direction × normal direction) is shown in Fig.1. Remarkably, BM microstructure consists of a large quantity of elongated grains and a minor fraction of fine equiaxed grains without twins. The AZ31 sheet with nominal gage dimensions of 300 mm (rolling direction, RD) × 100 mm (transverse direction, TD) × 6 mm (normal direction, ND) were prepared for welding. A cylindrical stir tool with thread pin (φ5 mm×5.7 mm) was used. After mechanical grinding, AZ31 Mg alloys were subjected to FSW along RD at a rotation rate of 1 400 rpm and a welding speed of 200 mm/min. Annealing treatment was performed on FSW materials with different annealing temperatures (150-300 ℃) and annealing time (15-120 min). Then several FSW materials and annealed materials are deformed to ε=3% (engineering strain). Dog bone-shaped samples (Fig.2) for tensile testing (along TD) were prepared from FM and AM. The transverse tensile testing was performed at room temperature with a strain rate of 0.001 s^{-1}.

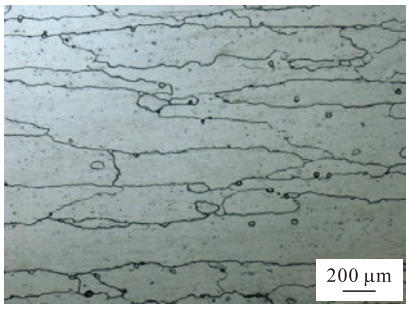

Fig.1 Original microstructure of die-casting AZ31 Mg alloy

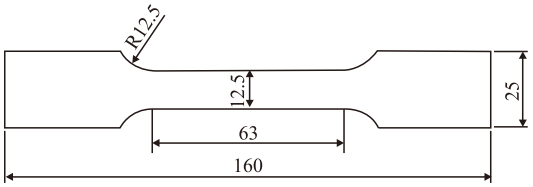

Fig.2 Dimensions of the tensile samples (unit: mm)

The samples obtained from FM and AM were sectioned along plane of TD×WD (RD) and their microstructure was analyzed by optical microscopy (OM), electron backscatter diffraction (EBSD). Before OM observation, those samples were grinded, polished and etched for 8 s with a solution (10 mL acetic acid, 10 mL distilled water, 4.2 g picric acid and 100 mL ethanol). The samples for EBSD analysis were electrolytic polished using a commercial AC2 Struers polishing solution at 38 V and ambient temperature. The EBSD test was employed using a ZEISS ULTRA 55 field-emission scanning electron microscopy with the step size of 0.8 μm and 1.0 μm. Then, the results were analyzed by HKL Channel 5 software.

3 Results and discussion

3.1 Microstructure of FSW sample

Schematic illustration of transverse cross section of FSW joint is shown in Fig.3. The retreating side (RS) is on the left and the advancing side (AS) is on the right. Due to different plastic flow and heat exposure in different zone, the joint may be divided into several regions: BM, thermo-mechanically affected zone (TMAZ), stir zone (SZ), and crown zone (CZ). Attempting to reveal microstructure evolution during FSW of magnesium alloys, several selected specific regions are given in Fig.3: position 1, SZ-center; position 2, SZ-middle; position 3, SZ-side; position 4, TMAZ/

SZ interface on AS; position 5, TMAZ. Corresponding EBSD maps and misorientation angle distribution of FSW joint are shown in Fig.4. High-angle grain boundaries (HABs) and low-angle grain boundaries (LABs) are depicted as black and yellow lines, respectively. In addition, the grains are colored according to their crystallographic orientation relative the WD.

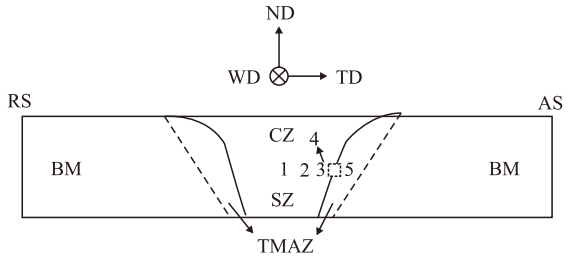

Fig.3 Schematic illustration of transverse cross section for FSW AZ31 Mg alloy

The microstructure of the SZ consists of recrystallized grains (Figs.4(a)-4(c)), but recrystallization degree gradually decreases from position 1 to position 3. The average grain size of position 1-3 in Fig.3 is shown in Table 1. In position 1, the full recrystallized and refined microstructure was observed and the average grain size was 7.68 μm (Fig.4(a)). This is because that SZ-center has higher temperature and flow stress during welding process, which accelerates nucleation of dynamic recrystallization (DRX). During dynamic recrystallization process, original grain boundaries provide favorable nucleation position by bulge behavior, as shown by black arrows in Fig.4(a). With removing from position 1 to position 3 in SZ, the recrystallization degree decreased and the average grain size increased to 10.17 μm (as shown in Fig.4(f)). Meanwhile, a few of twins occurred in recrystallized regions. On the basis of misorientation angle distribution (Fig.4(f)), it is found that the volume fraction of HABs ranging from

Table 1 The average grain size of position 1-3 in Fig. 3

Position	1	2	3
Average grain size	7.68 μm	9.01 μm	10.17 μm

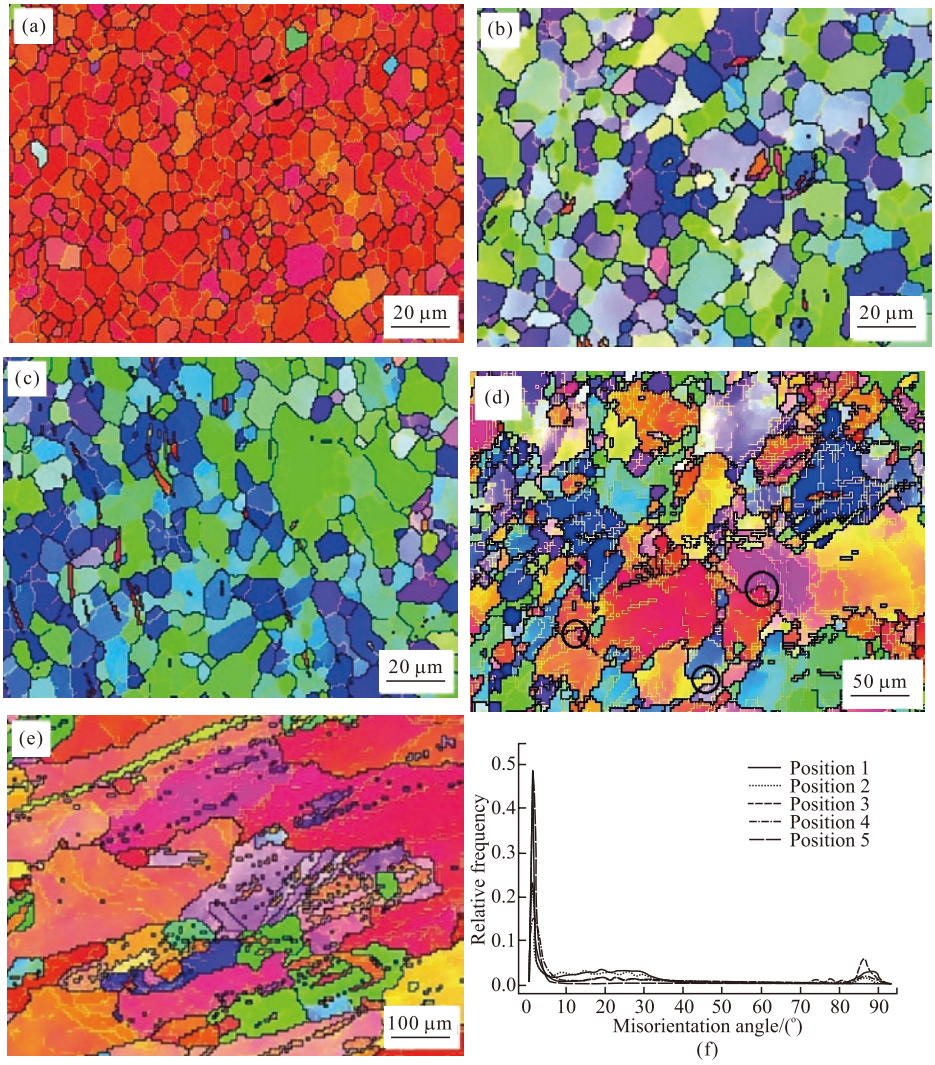

Fig.4 IPF maps of various regions (marked in Fig.2) in weld of FSW sample: (a) SZ-center; (b) SZ-middle; (c) SZ-side; (d) TMAZ/SZ interface on AS; (e) TMAZ; (f) the corresponding evolution of misorientation distribution

10° to 35° is higher in position 1 and position 2, which are 0.60 and 0.54, respectively. For position 3, the volume fraction of HABs ranging from 10° to 35° is 0.23, but the volume fraction of HABs about 86° obviously increased, as shown in Fig.4(f). It is very possible that higher deformation energy and heat input are produced by stirring pin, which improves DRX progress and accelerates transformation from LABs to HABs. As a result, the grain is effectively refined in SZ center. However, another interest point is that extensive (10-12) twins (about 86°) are found in position 3 of SZ-side, which is because that the heat input in this region is lower and DRX is depressed. Therefore, twinning gradually became another deformation coordination mechanism[20]. The non-uniformity of microstructure increased and several (10-12) twins and a great deal of LABs are found in original grain interiors in position 4 and position 5, as shown in Figs.4(d) and 4(e). In position 4, material experiences larger plastic deformation than that in position 5. A large quantity of refined recrystallization grains can be observed in TMAZ/SZ interface on AS. However, Fig.4(e) shows that no pronounced variations were found in grain morphology compared with the BM microstructure (Fig.1). It is because that plastic deformation and temperature in this zone are lower than that in the stir zone, which is not enough to stimulate nucleus for dynamic recrystallization. Therefore, the distortion energy was been stored by high density dislocation and the volume fraction of LABs is very high, as shown in Fig.4(f). As mentioned above, the grain refinement mechanism in FSW joint is complex and it is associated with continuous recrystallization, discontinuous recrystallization and twinning[21-23].

As shown in the above IPF maps, the microstructure in different positions of FSW joint has different crystal orientation. As we all know, different crystal orientation has different plastic deformation ability during deformation process. Therefore, we studied texture distribution and the corresponding (0001) and (11-20) pole figures as shown in Fig.5. The SZ has the most strong texture intensity and (0001) basal plane is perpendicular to WD. With the position moving from SZ to TMAZ, the intensity of (0001) texture dramatically reduced and the *c*-axis of most grains tilted from WD to TD, which is in line with previous studies[24-25]. It should be noted that the character of inhomogeneous microstructure and rich LABs in interface between TMAZ and SZ on AS may lead to severe stress concentration during transverse tensile testing, which increases the probability of fracture initiation in this position. In addition, due to the special texture with c-axis nearly parallel to TD in position 3, the activation of basal slip in this position is hardly achieved. Therefore, in attempting to reduce stress concentration in position 3 and 4 during transverse tensile testing, post-annealing treatment was conducted and its effect on microstructure evolution will be discussed in next section.

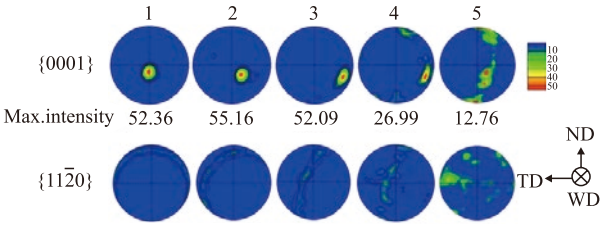

Fig.5 The (0001) and (11-20) pole figures showing texture distribution of the different zones in Fig.4

3.2 Microstructure of annealed samples

Fig.6 shows the microstructure in TMAZ/SZ interface of FSW and annealed samples. In all cases, the microstructure in this region consists of coarse elongated grains and refined equiaxed grains. There is no gradual transition from coarse matrix grains to fine grains, while the clear interface (as shown by straight line) between matrix grains and recrystallized region was observed in Fig.6(a), which may be one of the main reasons for breaking around this interface. However, the interfacial transition zone (ITZ) was observed after annealing treatment, as shown in Figs.6(b)-6(d). For example, after annealing at 150 ℃ for 60 min (Fig.6(b)), a quantity of equiaxed grains nucleate around original grain boundary and gradually grow into

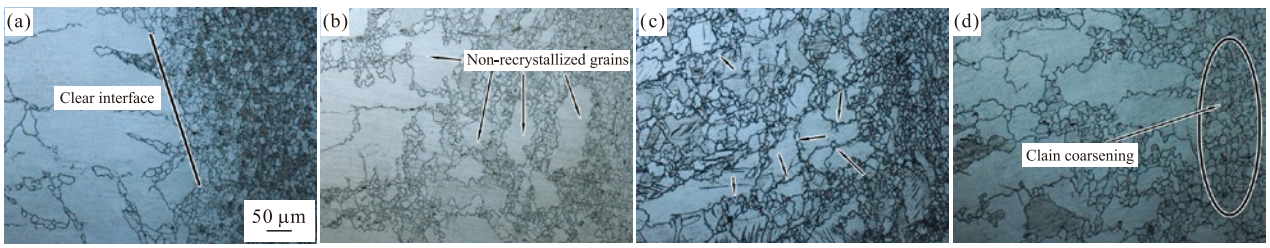

Fig.6 Optical micrographs of TMAZ/SZ interface on AS of different samples (a) FSW and annealed at (b) 150 ℃/60 min, (c) 200 ℃/60 min, and (d) 300 ℃/60 min

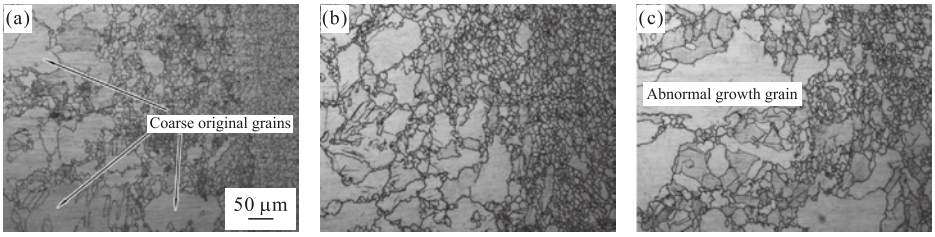

Fig.7 Optical micrographs of samples annealed at 200 ℃ for different times (a) 15min (b) 30min and (c) 120min

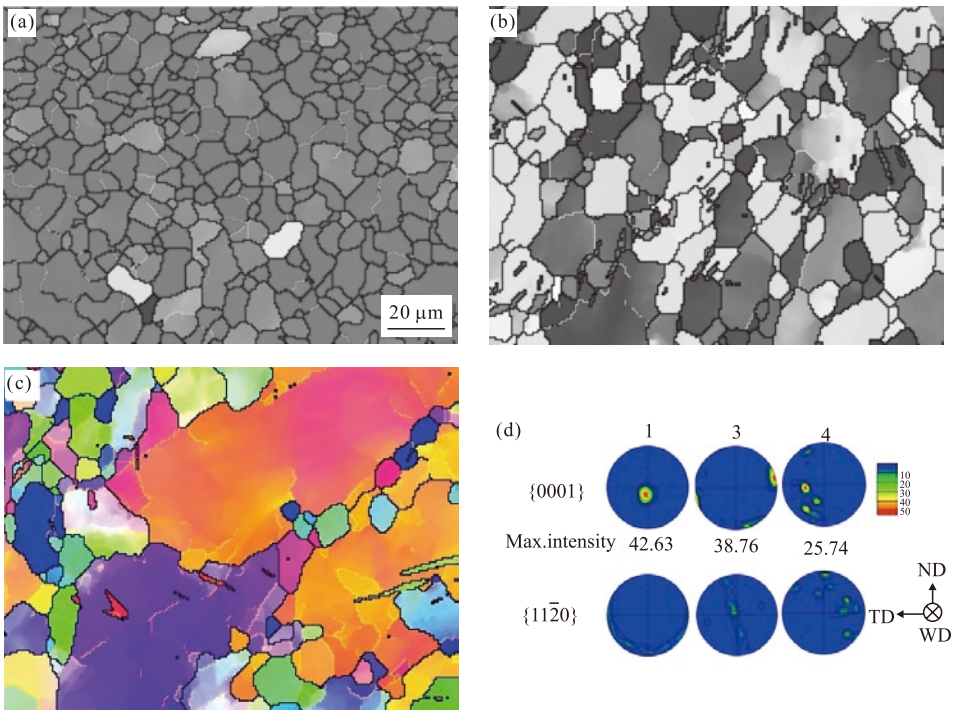

Fig.8 EBSD maps of various regions in FSW sample after annealing at 200 ℃ for 30 min: (a) SZ-center; (b) SZ-side; (c) TMAZ/SZ interface on AS and (d) the corresponding pole figures. In the maps, the grains are colored according to their crystallographic orientation relative the WD

matrix grains, which weakens drastic transition in this zone. It is because that annealing treatment promotes static recovery and static recrystallization of deformed grains, which is in good agreement with previous studies[19,26]. However, some non-recrystallized grains were still observed in this zone (as shown by arrows), which is due to the lower annealing temperature. After annealing at 200 ℃ for 60 min (Fig.6(c)), this interface shows more homogeneous microstructure with most of grain size less than 80 μm. In addition, more necklace-type grains are clustered along original grain boundaries (as shown by arrows). However, annealing treatment at 300 ℃ for 60 min results in grain coarsening, especially of the original fine grains adjacent to AS (Fig.6(d)). Fig.6 indicates that more homogeneous microstructure can be obtained by annealing at 200 ℃.

To investigate the effect of annealing time on the microstructure evolution in this interface, several FSW samples are treated at 200 ℃ for different times (15, 30, and 120 min) and its optical micrographs can be seen in Fig.7. It is found that coarse original grains (exceeding 100 μm) can be found in this interface after annealing at 200 ℃ for 15 min (Fig.7(a)), which indicates that static recovery and static recrystallization in this annealing condition are negligible. When the annealing time increased to 30 min, the degree of static softening increased and some recrystallized grains occurred along bulged original boundaries with higher stored energy, as shown in Fig.7(b). The microstructure is more homogeneous than that of sample treated at 200 ℃ for 60 min (Fig.6(c)). When the annealing time increased to 120min, pronounced grain coarsening and abnormal growth grains were observed in Fig.7(c). Although annealing treatment can improve recrystallization and microstructure distribution, excessive annealing temperature or holding time can lead to grain growth and coarsening. In short, more uniform microstructure was obtained by annealing at 200 ℃ for 30 min.

Attempting to clearly reveal the effect of annealing treatment on the changes of microstructure and texture, EBSD maps and corresponding pole figures of the sample annealed at 200 ℃ for 30 min are shown in Fig.8. After annealing, it is found that the average grain size of SZ-center and SZ-side increases from 7.5 μm and 9.8 μm to 8.6 μm and 13.6 μm, respectively. The number of LAGs reduced and moderate grain coarsening by annealing treatment is achieved by recovery accompanied with consuming of dislocations produced by FSW, as shown in Fig.8(a) and 4(a). Compared to Fig.4(c), the microstructure in Fig.8(b) is characterized by more uniform equiaxed grains and the fraction of LABs decreases from 0.40 to 0.26. A few (10-12) tension twins are also observed in SZ-side, which indicate that twins are hardly eliminated after annealing treatment. By comparing Fig.8(c) with Fig.4(d), only a few of LABs were observed and more static recrystallized grains formed along original coarse grain boundaries in TMAZ/SZ interface after annealing. The corresponding pole figures of various positions in the sample after annealing at 200 ℃ for 30 min are shown in Fig.8(d). It is found that the intensity of (0001) texture significantly reduced and a dispersive texture with the c-axis along ND was formed after annealing, which is in line with the study that heat treatment can reduce the intensity of basal texture of deformed magnesium alloy[27]. It indicates that appropriate annealing treatment may tailor deformed texture and improve plasticity of FSW Mg alloy joint.

3.3 Tensile properties

Fig.9 shows the typical engineering stress-strain curves of FSW sample and annealed samples. The details of tensile properties is summerizes in Table 2. There is no obvious difference in the shape of the engineering stress-strain curves between welded and annealed samples. From Fig.9(a), it can be seen that the annealing treatment can improve mechanical property of FSW Mg alloy joints. The annealing temperature had negligible effect on tensile strength and obviously enhanced plasticity of joints. This should be due to that the welding stress was released and homogeneity of microstructure was optimized during annealing process. The annealing treatment at 200 ℃ for 60 min can increase the elongation to 11.4% from 7.5% (welded sample). In order to study effect of annealing time on mechanical property, the tensile tests of samples annealed for different time were conducted and the results can be seen in Fig.9(b). It is found that the elongation gradually reduced and the strength slowly increased with increasing of annealing time. When annealing time increased from 15 min to 120 min, the yield strength and ultimate tensile strength increased from 126 MPa and 237 MPa to 164 MPa and 257 MPa, respectively, while elongation reduced from 13.4% to 9.3%. By analyzing of variation tendency of the stress-strain curves, it indicates that annealing treatment at 200 ℃ for 30 min can obtain better comprehensive mechanical property, *i e*, strength increased slightly and plasticity doubled approximately.

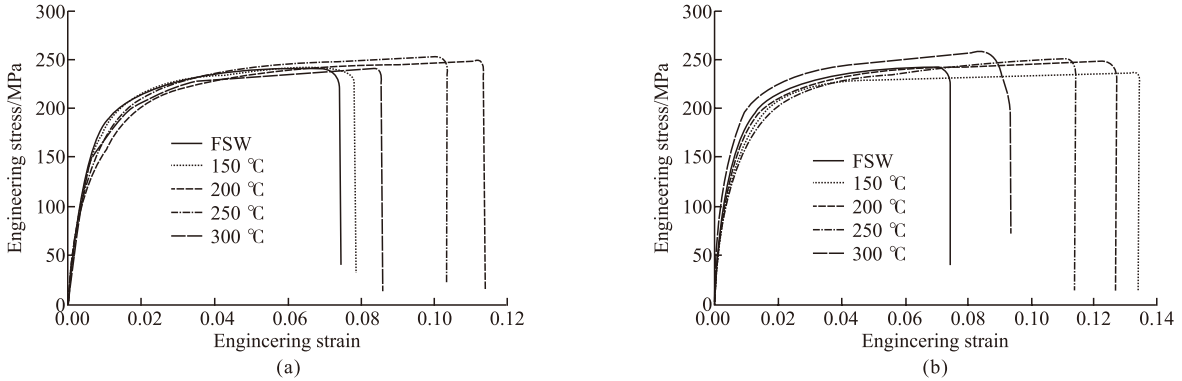

Fig.9 Engineering stress-strain curves of FSW sample and annealed samples at different conditions: (a) annealed at different temperatures for 60 min; (b) annealed at 200 ℃ with different holding time

Table 2 The details of tensile properties for FSW and annealed samples. In Table, yield strength, ultimate tensile strength and elongation are referred to YS, UTS, and EI, respectively

Tensile properties	FM	200 ℃ 15 min	200 ℃ 30 min	200 ℃ 60 min	200 ℃ 120 min	150 ℃ 60 min	250 ℃ 60 min	300 ℃ 60 min
YS/MPa	146	126	144	125	164	144	133	136
UTS/MPa	241	237	248	248	257	241	252	241
EI/%	7.5	13.4	13.0	11.4	9.3	7.8	10.3	8.6

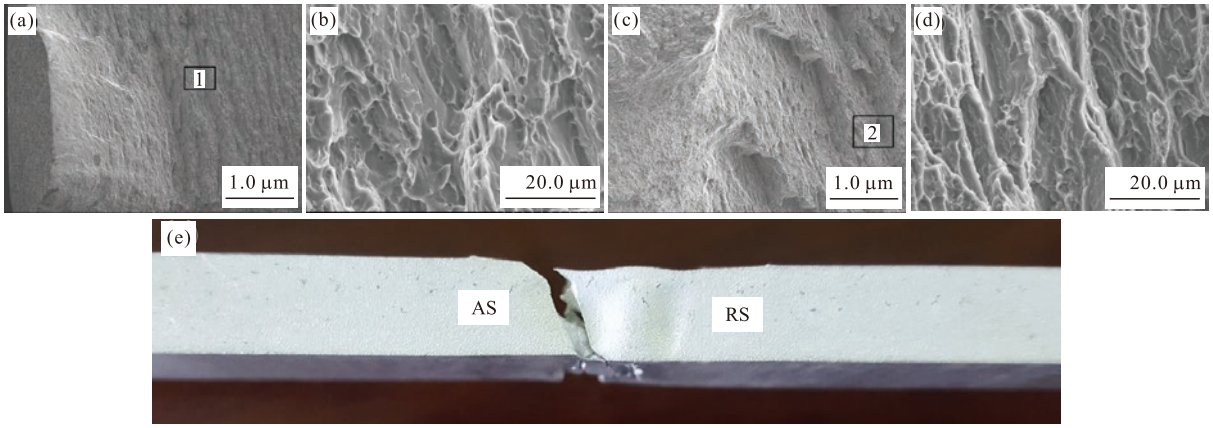

Fig.10 SEM morphologies of tensile fracture surface: (a) FSW sample; (b) partial enlarged detail of the region 1; (c) annealed sample at 200 ℃ for 30 min; (d) partial enlarged detail of the region 2; (e) macrograph of sample after fracture

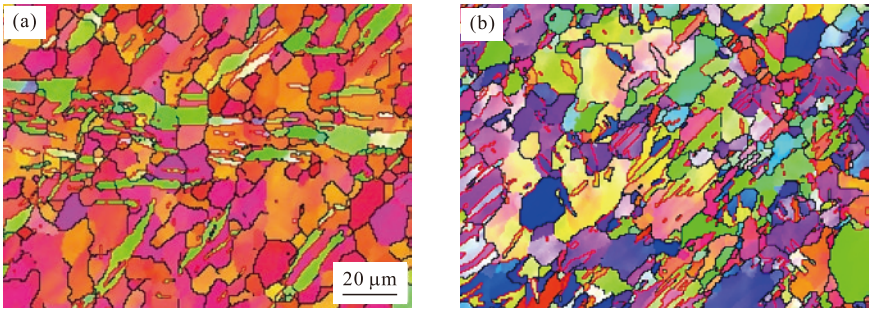

Fig.11 EBSD maps of various regions of 3% tensile samples: (a) SZ-side of FSW sample; (b) SZ-side of sample annealed at 200 ℃ for 30 min

Typical tensile fracture of FSW sample and annealed sample are shown in Fig.10. For FSW sample, the fracture surface is characterized by a single fracture slope and several relatively smooth tear ridges stretching along ND (Fig.10(a)). From partial enlarged detail of the region 1 in Fig.10(a) (Fig.10(b)), it can be seen that no dimples appeared around tensile fracture surface. The crack initiated and propagated along interface between TMAZ and SZ on AS, as shown in Fig.10(e). Previous study has reported that the main cleavage plane in HCP metals is the basal plane which has the lower critical fracture stress[28]. As mentioned above, we have demonstrated that the basal plane is almost perpendicular to TD in position 3 and position 4, as was shown in Fig.5. During tensile deformation, loading direction is perpendicular to basal plane in positions 3 and 4. As a result, basal slip is difficult to be activated during transverse tensile. In addition, inhomogeneity of grain size in interface is another key factor for crack formation. This is because that the ability to coordinate plastic deformation between coarse and fine grains is different[29]. Therefore, lower plasticity of FSW sample is significantly associated with severe basal texture distribution and microstructure inhomogeneity. However, after annealing at 200 ℃ for 30 min, intensity of deformed texture reduced and microstructure homogeneity was improved. Therefore, the annealed sample has better plasticity and its fracture morphology has complex fracture planes, as shown in Fig.10(c). In addition, compared to Fig.10(b), obvious surface relief are observed in Fig.10(d), which also indicates that sample annealed at 200 ℃ for 30 min has better plasticity than that of FSW sample. This conclusion is in line with the results discussed in Fig.9.

The increasing of plasticity of annealed sample may be attributed to the following factors. At first, pre-twins (10-12) (Fig.4(c) and Fig.8(b)) may give rise to crystal lattice rotation of 86.3° which can disperse severe basal texture in SZ-side and transform possible slip system from hard orientation to soft orientation. Therefore, twinning can motivate further slip of crystal and then increase plasticity of joint. A quality of residual stress is stored in the twin interior of deformed materials[30], and this accelerates elimination of twins during the subsequent tensile test, which may degrade the improvement of pre-twins on plastic deformation. It is well known that appropriate annealing treatment can pronouncedly release the residual stress stored in twins by static recovery and static recrystallization[19,26], which inhibits transformation of twins and retains its

Table 3 Averages of Schmid factor (SF) in position 3 of FSW and annealed samples

Average SF	Basal slip	Pyramidal slips	(10-12) twinning
FSW sample	0.342	0.095	0.401
Annealed sample	0.338	0.180	0.466

ability to coordinate deformation during tensile test. To clarify the effect of twin on plastic deformation, averages of Schmid factor (SF) in SZ-side of FSW and annealed sample (200 ℃/30 min) subjected to transverse tensile tests are calculated by EBSD statistical data and shown in Table 3. It is found that tension twinning is more favorable than basal slip in the SZ-side of FSW joint, this is in line with the previous studies[13]. Thus, twinning may be more easily activated during subsequent deformation. After annealing at 200 ℃ for 30 min, average SF of twinning increases, while average SF of slip decreases. It indicates that twinning is more likely to occur in annealed sample than that in FSW sample during tensile deformation, which is benefit of the increasing of joint plasticity. EBSD maps of FSW sample and annealed sample at 200 ℃ for 30 min deformed to 3% are shown in Fig.11. It has been calculated that the fraction of twins in SZ-side of FSW sample after deformation is about 15% (Fig.11(a)), while more twins (about 25%) are achieved for annealed sample subjected same deformation, as shown in Fig.11(b). It suggests that proper annealing treatment promotes twining which plays a predominant role for primary stage of plastic deformation in AS-side. Barnett *et al* also revealed that (10-12) twinning provides extension along the *c*-axis of hexagonal close packed lattice and improves uniform elongation during transverse tensile process[31]. On the contrary, annealing treatment cannot obviously enhance strength, which is because of elimination of dislocation and other substructures[32], seen in Fig.9. Secondly, the activation of pyramidal slips can improve plasticity of annealed joint. After annealing at 200 ℃ for 30 min, average SF of pyramidal slips increased, as shown in Table 3. It indicates that pyramidal slip plays a non-negligible role on plastic deformation of annealed sample during tensile. In addition, more uniform microstructure obtained by annealing is another important factor for improving plasticity. As aforesaid in section 3.2, appropriate annealing treatment can increase ITZ width and lead to gradual transition of grain size between the SZ and TMAZ. It is well known that dislocation diffusion rate is lower in coarse grains than that in fine grains. Thus, for the material consists of coarse grains and fine grains, more dislocations are clustered around grain boundaries of fine grains under tensile loading. This leads to local stress concentration around fine grains, which results in rapid fracture in those zones[29]. The annealed sample at 200 ℃ for 30min has more uniform microstructure distribution compared with FSW and other annealed samples, dislocations distribution becomes more dispersive during deformation, thus it exhibited better plasticity.

4 Conclusions

a) Annealing treatment at 200 ℃ for 30 min can obtain better comprehensive mechanical property. The elongation increased from 7.5% to 13.0% and strength increased slightly. The improvement of plasticity is due to formation of tension twins, increasing of microstructure homogeneity and activation of pyramidal slip.

b) Annealing treatment can inhibit twin transformation and retain its ability to coordinate deformation during subsequent tensile deformation. More deformation twins can be activated and obviously improved joint plasticity during tensile.

c) Annealing treatment can increase ITZ width and lead to gradual transition of grain size between the SZ and TMAZ, which balances dislocation diffusion rate in different zone. Moreover, SF value of pyramidal slip was increased after annealing treatment, which indicates that pyramidal slip also plays a non-negligible role on plastic deformation.

References

[1] Luo AA. Magnesium Casting Technology for Structural Applications[J]. *Jounal of Magnesium Alloys*, 2013, 1(1): 2-22

[2] Chen XP, Wang LX, Xiao R, *et al*. Comparison of Annealing on Microstructure and Anisotropy of Magnesium Alloy AZ31 Sheets Processed by Three Different Routes[J]. *Jounal of Alloys and Compounds*, 2014, 604(9): 112-116

[3] Taylor GI. Plastic Strain in Metals[J]. *Jounal of the Institute of Metals*, 1938, 62: 307-324

[4] Hector JLG , Trinkle DR , Yasi JA. First-principles Data for Solid-solution Strengthening of Magnesium: From Geometry and Chemistry to Properties[J]. *Acta Materialia*, 2010, 58(17): 5 704-5 713

[5] Zhao B, Debroy T. Pore Formation during Laser Beam Welding of Die-Cast Magnesium Alloy AM60B Mechanism and Remedy[J]. *Welding Journal Research Suppliment*, 2001, 204-210

[6] Yang J, Wang D, Xiao BL, *et al*. Effects of Rotation Rates on Microstructure, Mechanical Properties, and Fracture Behavior of Friction Stir-welded (FSW) AZ31 Magnesium Alloy[J]. *Metallurgical and Materials Transactions A*, 2013, 44(1): 517-530

[7] Mishra RS, Mahoney MW. Friction Stir Welding and Processing[J]. *Materials Science & Engineering R Report*s, 2005, 50(1-2): 1-78

[8] Templeman Y, Hamu GB, Meshi L. Friction Stir Welded AM50 and AZ31 Mg Alloys: Microstructural Evolution and Improved Corrosion

Resistance[J]. *Materials Characterization*, 2017, 126: 86-95

[9] Park SHC, Sato YS, Kokawa H. Effect of Micro-texture on Fracture Location in Friction Stir Weld of Mg Alloy AZ61 during Tensile Test[J]. *Scripta Materialia*, 2003, 49(2): 161-166

[10] Chang CI, Lee CJ, Huang JC. Relationship between Grain Size and Zener-Holloman Parameter during Friction Stir Processing in AZ31 Mg Alloys[J]. *Scripta Materialia*, 2004, 51(6): 509-514

[11] Suhuddin UFHR, Mironov S, Sato YS, *et al.* Grain structure evolution during friction-stir welding of AZ31 magnesium alloy[J]. *Acta Materialia*, 2009, 57(18): 5 406-5 418

[12] Mironov S, Onuma T, Sato YS, *et al.* Microstructure Evolution during Friction-stir Welding of AZ31 Magnesium Alloy[J]. *Acta Mateialia.*, 2015, 100: 301-312

[13] Liu DJ, Xin RL, Xiao Y, *et al*. Strain Localization in Friction Stir Welded Magnesium Alloy during Tension and Compression Deformation[J]. *Materials Science and Engineering A*, 2014, 609: 88-91

[14] Liu DJ, Xin RL, Yu HN, *et al*. Comparative Examinations on the Activity a Variant Section of Twinning during Tension and Compression of Magnesium Alloys[J]. *Materials Science and Engineering A*, 2016, 658: 229-236

[15] Chowdhury SH, Chen DL, Bhole SD, *et al*. Friction Stir Welded AZ31 Magnesium Alloy: Microstructure, Texture, and Tensile Properties[J]. *Metallurgical and Materials Transactions A*, 2012, 44(1): 323-336

[16] Liu DJ, Xin RL, Li ZY, *et al*. The Activation of Twinning and Texture Evolution during Bending of Friction Stir Welded Magnesium Alloys[J]. *Materials Science and Engineering A*, 2015, 646: 145-153

[17] Xin RL, Liu DJ, Xu ZR, *et al*. Changes in Texture and Microstructure of Friction Stir Welded Mg Alloy during Post-rolling and Their Effects on Mechanical Properties[J]. *Materials Science and Engineering A*, 2013, 582(11): 178-187

[18] Lee CJ, Huang JC, Du XH. Improvement of Yield Stress of Friction-stirred Mg-Al-Zn Alloys by Subsequent Compression[J]. *Scripta Materialia*, 2007, 56(10): 875-878

[19] Song B, Pan H, Chai LJ, *et al*. Evolution of Gradient Microstructure in an Extruded AZ31 Rod during Torsion and Annealing and Its Effects on Mechanical Properties[J]. *Materials Science & Engineering A*, 2017, 689: 78-88

[20] Qin FM, Zhu H, Wang ZX, *et al*. Dislocation and Twinning Mechanisms for Dynamic Recrystallization of As-cast Mn18Cr18N Steel[J]. *Materials Science & Engineering A*, 2017, 684: 634-644

[21] Mohan A, Yuan W, Mishra RS. High Strain Rate Superplasticity in Friction Stir Processed Ultrafine Grained Mg-Al-Zn Alloys[J]. *Materials Science & Engineering A*, 2013, 562: 69-76

[22] Yuan W, Mishra RS, Carlson B, *et al*. Material Flow and Microstructural Evolution during Friction Stir Spot Welding of AZ31 Magnesium Alloy[J]. *Materials Science & Engineering A*, 2012, 543: 200-209

[23] Wang XH, Wang KS. Microstructure and Properties of Friction Stir Butt-welded AZ31 Magnesium Alloy[J]. *Materials Science & Engineering A*, 2006, 431: 114-117

[24] Shan Q, Ni DR, Xue P, *et al*. Improving Joint Performance of Friction Stir Welded Wrought Mg Alloy by Controlling Non-uniform Deformation Behavior[J]. *Materials Science & Engineering A*, 2017, 707: 426-432

[25] Xin RL, Liu DJ, Shu XG, *et al*. Influence of Welding Parameter on Texture Distribution and Plastic Deformation Behavior of As-rolled AZ31 Mg alloys[J]. *Journal of Alloys & Compounds*, 2016, 670: 64-71

[26] Fong KS, Danno A, Tan MJ, *et al*. Tensile Flow Behavior of AZ31 Magnesium Alloy Processed by Severe Plastic Deformation and Post-annealing at Moderately High Temperatures[J]. *Journal of Materials Processing Technology*, 2017, 246: 235-244

[27] Kim WJ, Jeong HG, Jeong HT. Achieving High Strength and High Ductility in Magnesium Alloys Using Severe Plastic Deformation Combined with Low-temperature Aging[J]. *Scripta Mateialia.*, 2009, 61(11): 1 040-1 043

[28] Ovid'ko IA, Langdon TG. Enhanced Ductility of Nanocrystalline and Ultrafine-grained Metals[J]. *Reviews on Advanced Materials Science*, 2012, 30: 103-115

[29] Yoo MH. Slip, twinning, and Fracture in Hexagonal Close-packed Metals[J]. *Metallurgical and Materials Transactions A*, 1981, 12(3): 409-418

[30] Wu L, Agnew SR, Brown DW, *et al*. Internal Stress Relaxation and Load Redistribution during the Twinning-detwinning-dominated Cyclic Deformation of a Wrought Magnesium Alloy ZK60A[J]. *Acta Materialia*, 2008, 56(14): 3 699-3 707

[31] Barnett MR. Twinning and the Ductility of Magnesium Alloys Part I: "Tension" Twins[J]. *Materials Science & Engineering A*, 2007, 464(1): 1-7

[32] Liu Z, Xin RL, Wu X, *et al*. Improvement in the Strength of Friction-stir-welded ZK60 Alloys Via Post-weld Compression and Aging Treatment[J]. *Materials Science & Engineering A*, 2018, 712: 493-499